Measurement of Defect Energy Level in MgO Layer

***Chang. Gil. Son**, K. B. Song, S. J. Jeoung, E. Y. Park, J. S. Kim*, S. J* and E. H. Choi*

Charged particle beam and plasma laboratory / PDP Research Center, Department of Electrophysics
Kwangwoon University, 447-1, Wolgye-Dong, Nowon-Gu, Seoul, Korea

***C&Chem, Korea**

wizardog@naver.com, Phone : +82-2-940-5662, Fax : +82-2-913-6187

Abstract

The secondary electron emission coefficient (γ) of the cathode is an important factor for improving the discharge characteristics of AC-PDP, because of its close relationship to discharge voltage. In this experiment, we have investigated the electronic structure of the energy band in the MgO layer responsible for the high γ. We used three kinds of MgO pellet that have another component, and each MgO layers have been deposited by electron beam evaporation method. The work-functions of MgO layer have been investigated from their ion-induced secondary electron emission coefficient (γ), respectively, using various ions with different ionization energies in a γ-FIB (Focused Ion Beam) system. We have compared work-function with γ-FIB system current signal for measurement defect energy level in MgO layer. MgO-A in the three types has lowest work-function value (4.12eV) and there are two defect energy levels.

1. Introduction

The MgO protective layer is an important element of AC-PDP. This thin film protects the dielectric layer above the electrodes from sputtering while at the same time yielding a high ion-induced secondary electron emission coefficient (γ) [1]. Because of its large secondary electron emission coefficient, the MgO protective layer plays an essential role in keeping the breakdown voltage relatively low.

MgO layer potential electron emission is the important source that supply secondary electron in discharge area, as the average energy of the ions are very small (~eV) in AC-PDP. The relevant mechanisms are Auger neutralization and resonance neutralization followed by Auger de-excitation. Fig. 1 shows a schematic diagram of the Auger neutralization process.

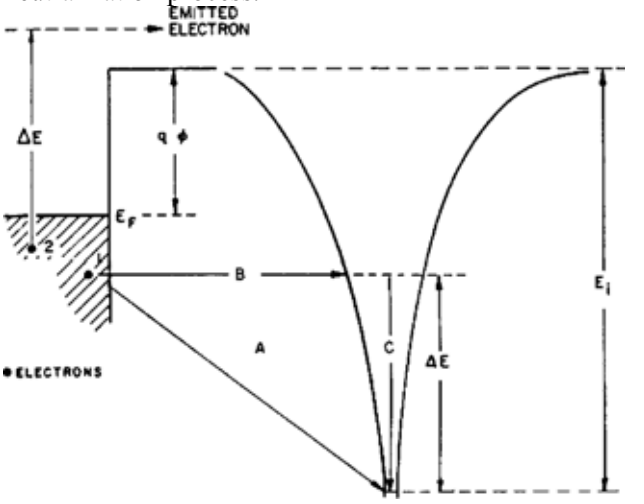

Fig. 1 Schematic diagram of the Auger neutralization process

As an ion with ionization energy E_i approaches the insulator surface, it undergoes a neutralization process whereby one electron in the valence band of the insulator is captured by the ion. The Auger transition implies that the energy gained by this neutralization process is simultaneously used to excite a second electron to a higher energy level. If it exceeds the surface barrier energy E_o the excited electron can escape from the surface and becomes a secondary electron. The maximum kinetic energy of the secondary electrons ejected is given by

$$E_{kmax} = E_i - 2(E_g + \chi)$$

χ is the electron-affinity, E_g is the band gap energy of the solid, and E_i is the ionization energy of the gas ion. It is reported that the theoretical gamma values of MgO without defect energy bands in the band gap for Kr and Xe ions become zero from Hagstrum's theory. But MgO with defect energy bands in the band gap affects work function and secondary electron

emission. And the γ of MgO with defect energy band in the band gap was calculated theoretically for Kr and Xe ions [3][4]. Also, we can measure γ of MgO for Xe ions by using γ -FIB system. We thought that these energy bands by defect state are affected MgO component. It is reported that the Cathode-luminescence spectra that has relation to the energy bands depend on these factor [6]. When we have measured secondary electron coefficient (γ) by γ-FIB system, we have observed the current signals that have step shape, where the defect states are assumed. It is observed that energy level by the defect state of MgO layer exists between conduct band and valence band.

2. Experimental Configuration

In this experiment, we used three kinds of MgO pellet that have another component, and deposited 500nm on ITO (Indium Tin Oxide) glass. Each MgO layers have been deposited by electron beam evaporation method under evaporation rate 5 Å/s, thickness 7000 Å, substrate temperature 200 ℃, and vacuum annealing process at 300 ℃ during 30 min. These samples were lorded γ-FIB system and we used four kinds of gas (He, Ne, Ar, Xe) for work-function measurement.

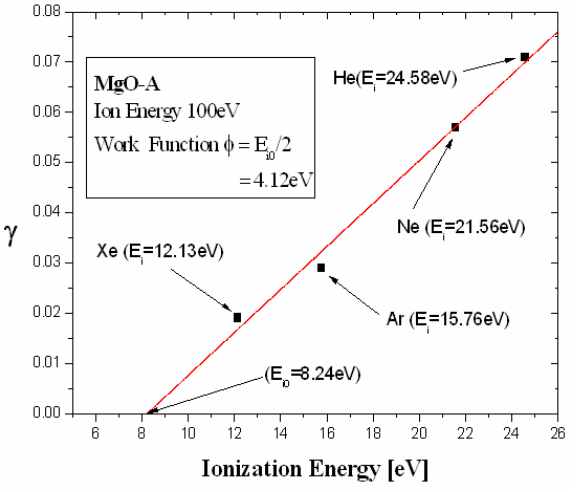

Fig. 2 Measurement of work function of MgO-A layer by γ-FIB system

For schema of electron structure including energy bands by defect state of MgO layer, the current signal of MgO layer versus collect voltages is obtained for Ne gases by γ -FIB system. As seen in the Figs. 2 and 3, we have calculated work function and defect energy between energy bands in energy gap of MgO layer. As a result, we obtained the electronic structure diagram of MgO layer, as Fig. 4. If the first defect energy band is nearer the conduction band then MgO layer has lower work function and higher γ.

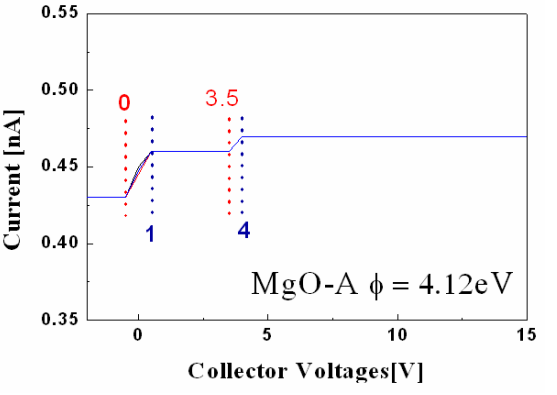

Fig. 3 Current signal at point of converting ion current into total current which is sum of ion current and secondary electron current of MgO layer versus collect voltage

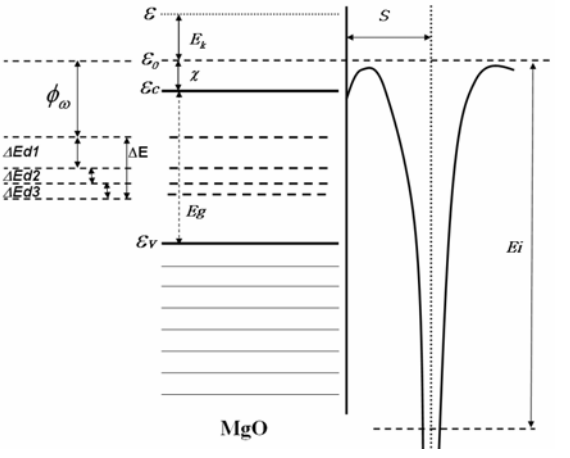

Fig. 4 Schematic diagram of electronic structure including energy band in energy gap of MgO layer

3. Experimental result

We have measured the γ of each MgO layer, work function and total current signal which includes the ion and secondary electron current. Fig. 5 shows the secondary electron emission coefficient that

accordance with kinds of MgO. MgO-A is obviously found to have the highest ion-induced secondary electron emission coefficient (γ) from 0.035 up to 0.134, while from 0.014 to 0.098 for MgO-B and from 0.01 to 0.072 for MgO-C for Ne ions whose acceleration voltage ranges from 100 to 200 V throughout this experiment. Table 1 noted that the work function ϕw for MgO-C is shown to be the highest value 5.34 eV, while it is 4.25 eV for MgO-B the lowest value of 4.12 eV for MgO-A.

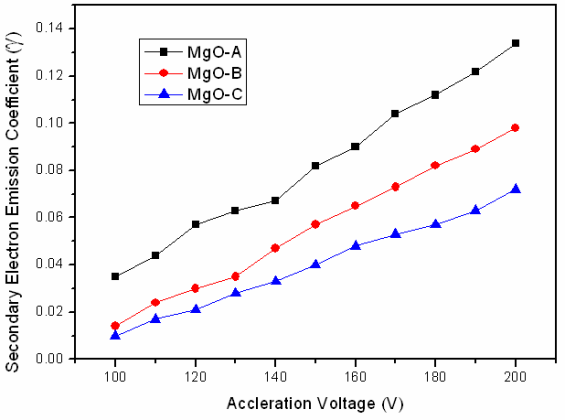

Fig. 5 Secondary electron emission coefficient (γ) which follows in MgO types

MgO types	MgO-A	MgO-B	MgO-C
Work function (φ)	4.12 eV	4.25 eV	5.34 eV

Table 1. Work function (φ) which follows in MgO types

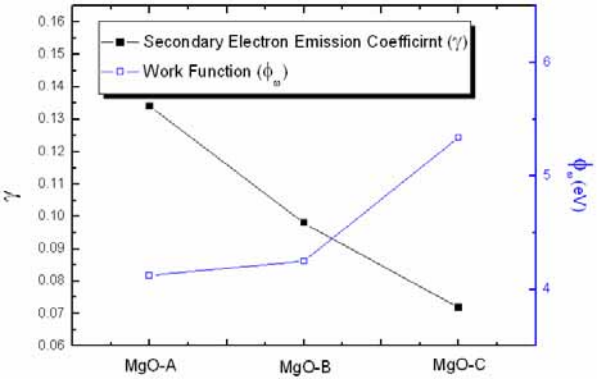

Fig. 6 Ne ion induced secondary electron coefficient (γ) designated by solid squares and work function φ_w by open squares from MgO types

Fig. 6 shows the results of the work functions φ_w from MgO types, respectively, designated by the open squares, along with the ion-induced secondary electron emission coefficient (γ) for Ne ion of 100 eV by solid squares. As you see the figure, MgO-A has highest secondary electron emission coefficient and lowest work function.

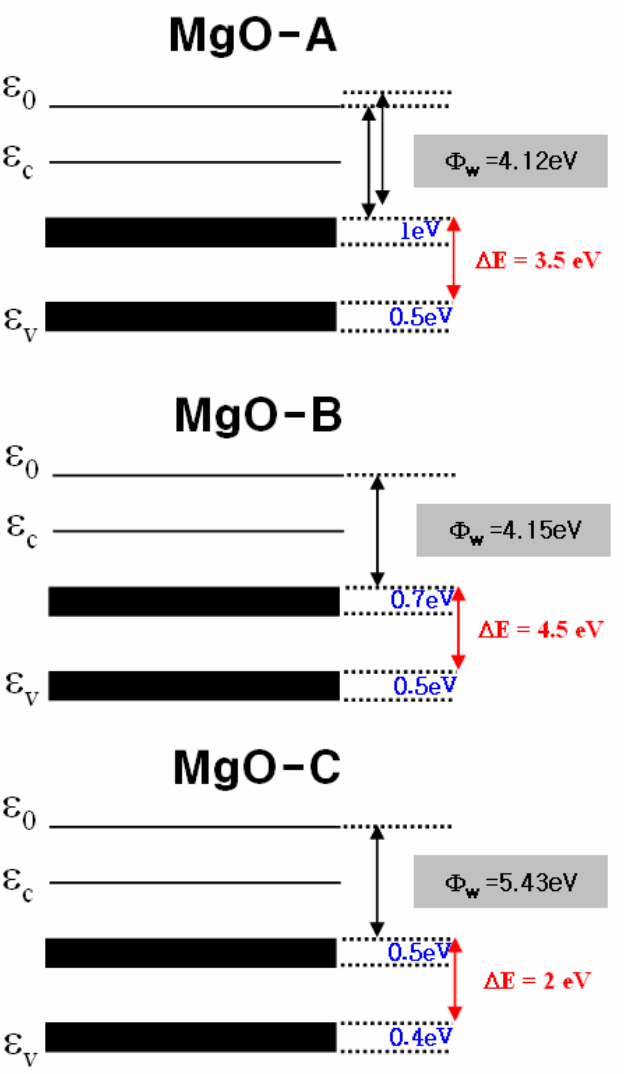

Fig. 7 Energy band including defect levels

These results showed that Each MgO component caused different secondary electron emission coefficient and work function. Also, as you see the fig. 7 each MgO layer has different energy band structure including defect levels. These energy band distributions relate high secondary electron emission

coefficient (γ) and improvement of efficiency in AC-PDP. Hence, energy band measurement method is most important to understand MgO layer characteristics.

4. Conclusion

We know that dielectric protective layer with high secondary electron emission coefficient (γ) is an important factor in lowing breakdown voltage. We have investigated on the defect levels inside the MgO energy bands, which are assumed to be important to γ. So, we have approached and presented the electronic structure of defect energy levels in MgO protective layer according to MgO component. As a result, we have known that the defect levels give an influence on the secondary electron emission.

7. References

[1] J. P. Boeuf, J. Phys. D : Appl. Phys. 36 , p.66-70, (2003)

[2] J. H. Lee, J. H. Eun, S. Y. Park, S. G. Kim, H. J. Kim, Thin Solid Films 435, p.95-101, (2003)

[3] O. Engkvist, A. J. Stone, Surface Science 437, p.239-248, (1999)

[4] J. C. Jung, H. S. Jung, W. B. Park, E. H. Choi, J. W. Cho, IDW'04, p.764-769

[5] J. Y. Lim, J. S. Oh, B. D. Ko, J. W. Cho, S. O. Kang, G. S. Cho, H. S. Uhm, E. H. Choi, J. Appl. Phys. 94, p.764-769, (2003)

[6] H. D. Hagstrum, Phys. 96, 336, 1954

[7] H. D. Hagstrum, Phys. 122, 83, 1961

[8] Yasushi Motoyama, J. Appl. Phys., vol. 95 no. 12 , 2004

[9] Yasushi Motoyama and Fumio Sato, IEEE Transactions on plasma science, VOl. 34, No 2, April 2006

[10] Yasushi Motoyama, Yoshikuni Hirano at al., J. Appl. Phys., Vol. 95, No. 12, pp. 8419~8424, March 2004